Metal- and halide-free solid-type multifunctional alkanolamines as catalysts for cycloaddition of CO_2

Hyeon-Gook Kim[†], Hye Jeong Son, and Choong-Sun Lim

Advanced Industrial Chemistry Research Center, Advanced Convergent Chemistry Division,
Korea Research Institute of Chemical Technology, 45 Jongga-ro, Jung-gu, Ulsan 44412, Korea

Abstract–Although the production of cyclic carbonates from CO_2 and epoxides can be promoted by eco-friendly halogen- and metal-free organic catalysts, its homogeneity complicates the catalyst reuse. Herein, we synthesized solid multifunctional alkanolamines using simple epoxy and amine reactions, and analyzed their structures by IR and ^{13}C-NMR. Then, we employed these as catalysts for CO_2 cycloaddition with propylene oxide, obtaining propylene carbonate in 98% yield after 3 h at 120 °C. Moreover, at 60 °C, the reaction was successfully repeated five times and a product yield of 50% was maintained throughout.

Keywords: Alkanolamine, Carbon Dioxide Fixation, Metal- and Halide-free, Solid Catalyst, Propylene Carbonate
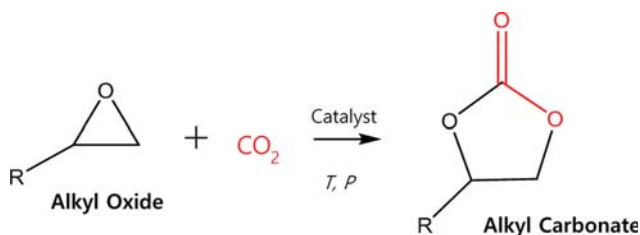
INTRODUCTION

Among the many environmental issues, global warming is mainly caused by the depletion of the ozone layer by greenhouse gases, eventually leading to an increase in the global average temperature. The use of indiscriminate fossil fuels leads to an excessive emission of greenhouse gases, thereby causing the greenhouse effect. The production of carbon dioxide (CO_2), which is considered to be the leading cause of the greenhouse effect, is continuously increasing owing to growing industrialization [1]. Carbon dioxide capture utilization (CCU), which relies on the use of CO_2 as a starting material for chemical reactions, has been introduced as a method to reduce the atmospheric content of greenhouse gasses. Among available CCU processes, the production of ethylene carbonate from ethylene oxide and CO_2 on a 200-million-ton/year scale is a prime example of a successful industrial approach [2]. For example, CCU plays an important role in the catalytic mechanism of a cycloaddition reaction, in which cyclic carbonate is formed from an epoxide and CO_2 (Scheme 1) [3-8].

Cyclic carbonates such as ethylene carbonate (EC) and propylene

Scheme 1. Synthesis of alkyl carbonate through a catalytic reaction between CO_2 and alkyl oxide.

[†]To whom correspondence should be addressed.
E-mail: candoit@krict.re.kr

carbonate (PC) are mainly used as aprotic polar solvents for Li-ion batteries as well as intermediates and precursors of pharmaceuticals and fine chemicals [9,10]. In the industrial synthesis of cyclic carbonates, metal halide salts such as LiBr and KI are often used as catalysts. When considering possible catalyst recycling, metal halide salts are very suitable since they can be dissolved in the cyclic carbonate that is formed from the reaction, and do not precipitate during the purification process [11]. Other reagents employed in the cycloaddition reaction between epoxides and CO_2 include homogeneous and heterogeneous catalysts including metal oxides [12], metal-organic frameworks [13,14], metal salts [15,16], transition metal complexes [17], ionic liquids [18,19], organic functionalized polymers [20], alkanolamine catalysts [21], solid catalysts [22], polymer catalysts [23], silver electrodes [24], and graphene/graphene oxides [25-28]. For commercial applications, heterogeneous catalysts are preferred over homogeneous catalysts, due to the ease of separation and reuse [29-31].

Solid-supported catalysts, in particular, have received an increased amount of attention, because they exhibit several advantages in preparative procedures, e.g., work-up simplification and catalyst separation and recycling [32]. Polymer-type solid catalysts have also been applied to CO_2 conversion reactions; however, excellent results could not be obtained. For example, in order to obtain a certain level of PO (propylene oxide) yield, metalloporphyrin-based organic polymers [33] require a reaction pressure of 30 bar and a co-catalyst, dicyandiamide-formaldehyde [34] needs a reaction pressure of 20 bar, NP-NHCs [35] requires a reaction time of 24 h, and the reaction with covalent triazine [36] is carried out under harsh conditions. In the case of multifunctional alkanolamine catalysts [21], it was suggested that the hydroxyl groups strongly bind epoxides, thereby facilitating their ring opening by bringing amine-bound CO_2 into close proximity. Moreover, the lone pair of electrons on the catalyst nitrogen atom is thought to interact with the electrophilic carbon of CO_2, causing the nucleophilic attack of the CO_2 oxygen atom on the alkyl oxide and allowing a subsequent ring opening [21].

In this study, four kinds of solid catalysts were prepared in an effort to address the issue of homogeneity. The experiments started with the idea that polymers could be formed from the reaction of an amine and epoxy and used as a catalyst. In fact, the aforementioned reaction yielded four polymeric solids consisting of tertiary amines and hydroxyl groups. It was assumed that due to their insolubility in various solvents, the solid catalysts crosslinked via epoxy and amine reactions to form gels. Furthermore, the four resulting polymers could actively convert CO_2 and PO even in the absence of metals and halogens, which was attributed to the fact that these polymers contain numerous multifunctional alkanol amine groups. In addition, we found that the polymers can be reused because they maintain the form of catalyst after the reaction.

MATERIALS AND METHODS

1. Chemicals and Reagents

CO_2 (99.999%, Korea Specialty Electronic Materials Co., Ltd., Yangsan, Korea) was used as obtained, without further purification. Propylene oxide (99%), glycerol diglycidyl ether (technical grade), piperazine (99%), tris(2,3-epoxypropyl) isocyanurate, tris(4-hydroxyphenyl)methane triglycidyl ether, and trimethylolethane triglycidyl ether were purchased from Sigma-Aldrich (Darmstadt, Germany)

and used without further purification.

2. Instruments

PO and PC were quantified using a gas chromatograph (450-GC, Bruker, Germany) equipped with a flame ionization detector and a capillary column (HP-5, 5% phenylmethyl polysiloxane, Agilent, Santa Clara, USA), using biphenyl as an internal standard. The catalyst structures were elucidated through ^1H NMR spectroscopic measurements (300 MHz, Avance DPX-400, Bruker, Germany), employing $CDCl_3$ as a solvent, and ^{13}C NMR analysis on a 400-MHz solid-state NMR spectrometer (Avance III HD, Bruker, Germany) at KBSI Western Seoul Center. For the Fourier transform infrared (FT-IR) analysis, disks formed from the samples at a pressure of 100 Pa were placed in a quartz cell with a KBr window (Nicolet 6700, Thermo Scientific, USA), scanning in the range of 700-4,000 cm^{-1}. The results from the FT-IR analysis are presented in the Supporting Information. Since the solid catalysts did not dissolve in any solvent, it was difficult to measure their molecular weights. After various attempts, the molecular weights of solid catalysts were measured using the MALDI-TOF/TOF^{TM} 5800 system (AB SCIEX), with a positive reflector operating mode and a mass range (m/z) of 1,000-3,000 Da. Three different MALDI matrices were prepared according to the literature and applied [37]: i) 2,5-dihydroxybenzoic acid (DHB): 10 mg/mL (water), ii) 2,5-dihydroxy-
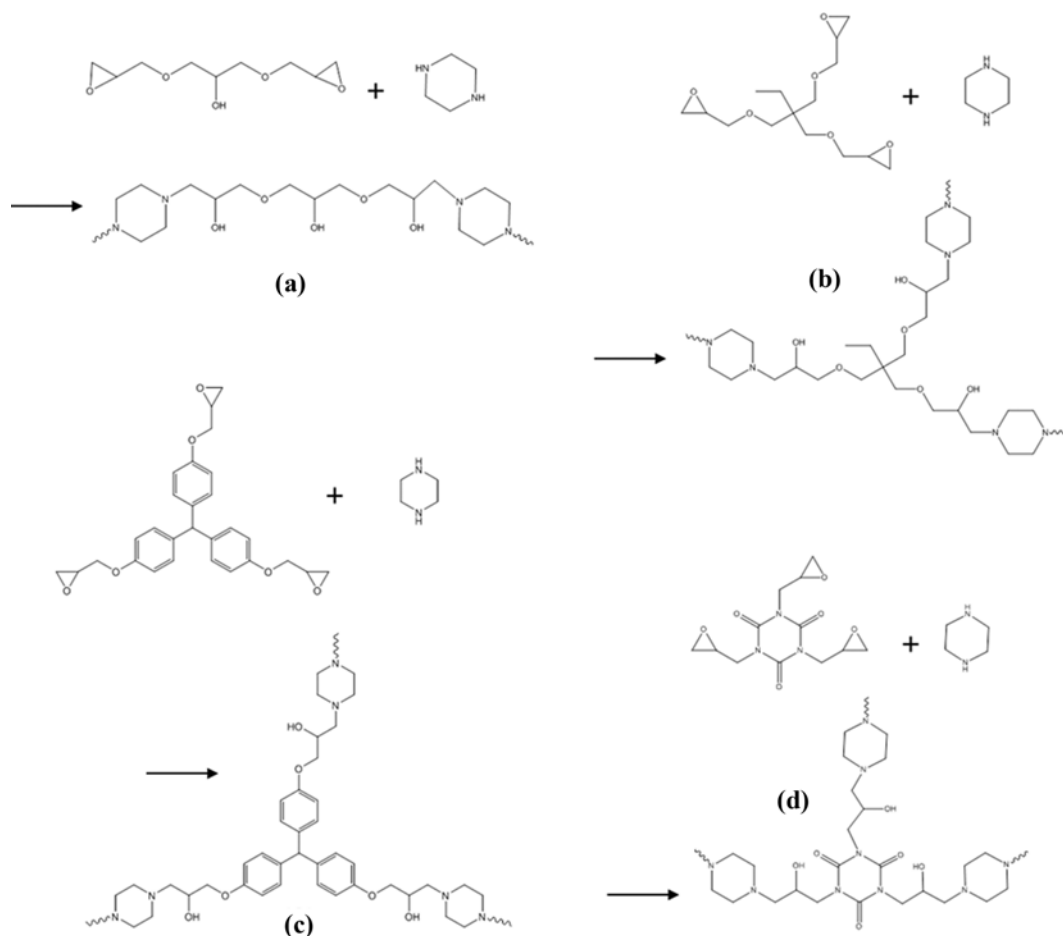

Fig. 1. Preparation scheme of solid type (a) catalyst 1 (piperazinediol) (b) catalyst 2 (triolpiperazine) (c) catalyst 3 (triphenylpiperazine) (d) catalyst 4 (cyanupiperazine).

benzoic acid (DHB): 10 mg/mL (THF), iii) dithranol: 10 mg/mL (THF/0.1% TFA). The results from the MALDI-TOF are presented in the Supplementary data (molecular weight: 1,200-2,500 g/gmol).

3. General Procedure for Catalyst Preparation

The respective starting material was added to ethanol and left to dissolve for 1 h. Then, piperazine (1.72 g) was added and the mixture was allowed to react for 12 h at room temperature. After the exothermic reaction was complete, the solvent was removed at 60 °C under vacuum and a white solid that did not dissolve in any solvent was obtained.

3-1. Specific Procedure for Piperazinediol

Piperazine diol was prepared according to the general procedure presented in section 3 with the use of glycerol diglycidyl ether (3.09 g) as a starting material. The catalyst structure is shown in Fig. 1(a) and a photo of the formed catalyst is shown in Fig. 2(a).

3-2. Specific Procedure for Triepoxypiperazine

Triepoxypiperazine was prepared according to the general procedure presented in section 3 with the use of trimethylolpropane triglycidyl ether (3.2 g) as a starting material. The catalyst structure is shown in Fig. 1(b) and a photo of the formed catalyst is shown in Fig. 2(b).

3-3. Specific Procedure for Triphenylpiperazine

Triphenylpiperazine was prepared according to the general procedure presented in section 3 with the use of tris(4-hydroxylphenyl)methane triglycidyl ether (4.6 g) as a starting material. The catalyst

Fig. 2. Picture of solid catalyst ((a) Piperazinediol, (b) triolpiperzine, (c) triphenylpiperazine, (d) cyanupiperazine).

structure is shown in Fig. 1(c) and a photo of the formed catalyst is shown in Fig. 2(c).

3-4. Specific Procedure for Cyanupiperazine

Cyanupiperazine was prepared according to the general procedure presented in section 3 with the use of tris(2,3-epoxyproyl) isocyanurate (2.97 g) as a starting material. The catalyst structure is shown in Fig. 1(d) and a photo of the formed catalyst is shown in Fig. 2(d).

4. Cycloaddition Reaction

For each typical batch operation, a stainless steel autoclave reactor (50 mL) equipped with a magnetic stirrer was charged with propylene oxide (5.0 g) and the catalyst of choice in the absence of any solvent, and purged with CO_2 several times, followed by room-temperature pressurization with CO_2 to 10 atm. The reaction was initiated at the target temperature upon stirring at 500 rpm. Since the catalysts were insoluble in PO and PC at the reaction temperature, their solubility did not affect the results. Once the reaction was complete, the reactor was cooled to room temperature and vented [21]. After the first reaction, a regeneration test was performed by filtering the catalyst using filter paper and vacuum drying it to completely remove the remaining PO and PC. Then, a second test was carried out in the same manner, using the regenerated catalyst.

RESULTS AND DISCUSSION

1. FT-IR Analysis of the Solid Catalysts

An infrared spectrum is commonly obtained by passing infrared electromagnetic radiation through a sample that possesses a permanent or induced dipole moment and determining what fraction of the incident radiation is absorbed at a particular energy. In an absorption spectrum, the energy of each peak corresponds to the frequency of the vibration of a molecular part, thus allowing the qualitative identification of certain bond types in the sample [38]. In this work, the FT-IR spectra of the solid catalysts (Fig. 3) confirmed the presence of functional groups. The characteristic peaks of the respective catalysts were as follows: i) for piperazinediol (Fig. 3(a)), those of the C-O stretching (1,102 cm^{-1}), C-N stretching (1,303 and 1,458 cm^{-1}), C-H stretching (2,821 and 2,916 cm^{-1}), and O-H stretching (3,370 cm^{-1}); ii) for triolpiperazine (Fig. 3(a)), those of the C-O stretching (1,097 cm^{-1}), C-N stretching (1,302 cm^{-1} and
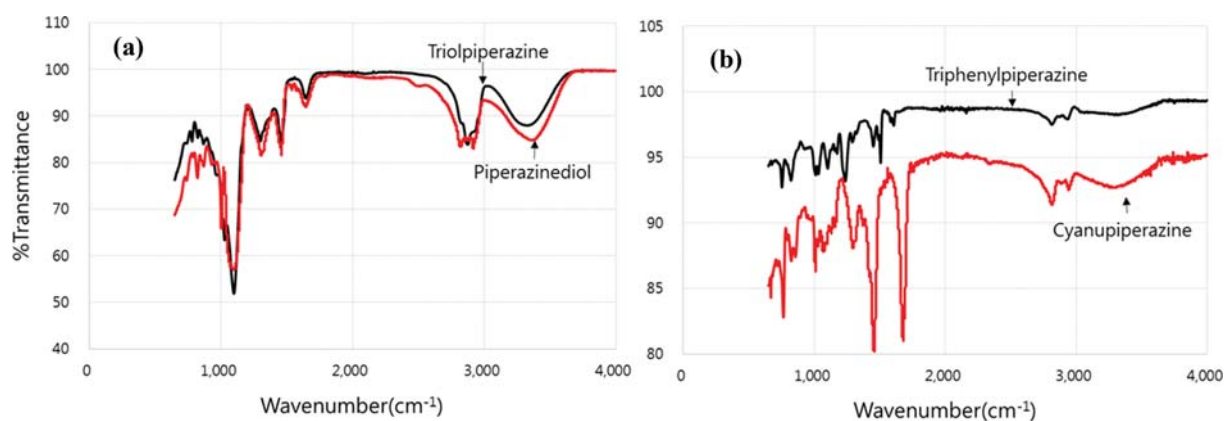

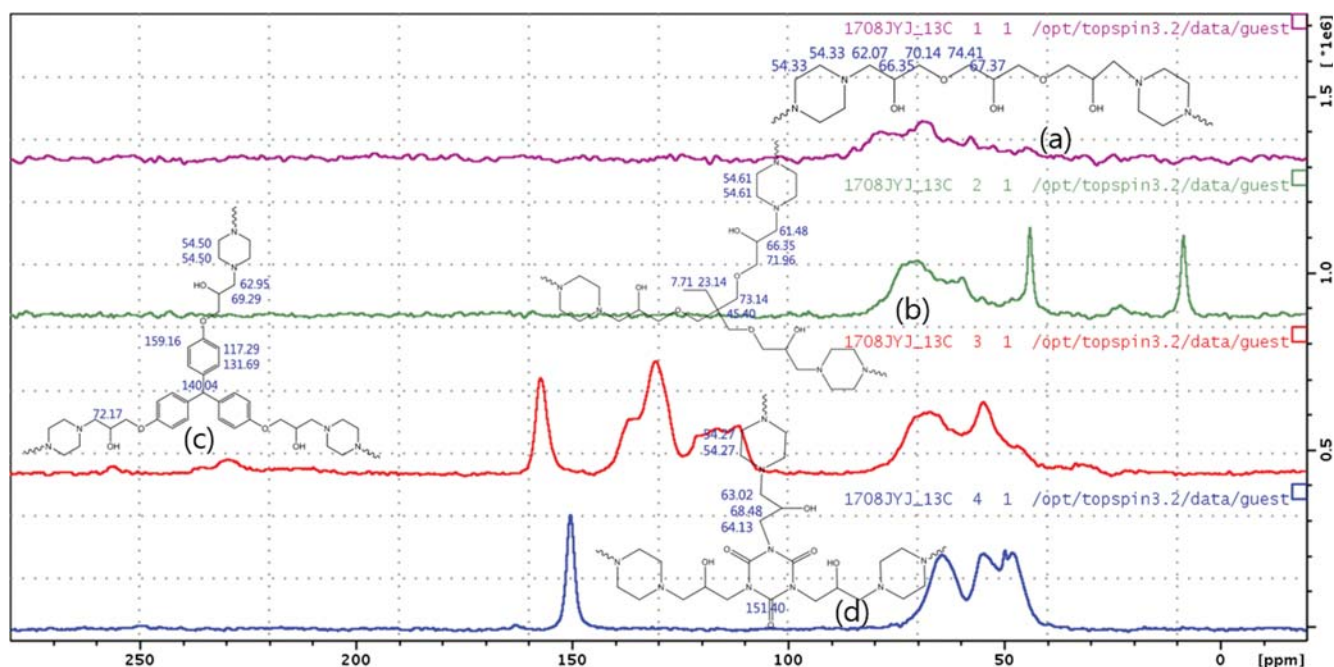**Fig. 3. FT-IR spectrum of the solid catalysts.**

Fig. 4. Solid state ^{13}C NMR NMR spectra of the catalysts ((a) Piperazine diol, (b) triol piperazine, (c) triphenylpiperazine, (d) cyanupiperazine).

1,458 cm^{-1}), C-H stretching (2,874 cm^{-1}), and O-H stretching (3,348 cm^{-1}); iii) for triphenylpiperazine (Fig. 3(b)), those of the Ar bending (753 cm^{-1} and 756 cm^{-1}), CO stretching (1,009 cm^{-1} and 1,238 cm^{-1}), CN stretching (1,501 cm^{-1}), C=C Ar (1,507 cm^{-1}), and CH stretching (2,816 cm^{-1} and 2,932 cm^{-1}); iv) for cyanupiperazine (Fig. 3(b)), those of the C-O stretching (1,009 cm^{-1}, 1,013 cm^{-1}), C=O stretching (1,679 cm^{-1}), C-H stretching (2,817 cm^{-1}, 2,945 cm^{-1}), and O-H stretching (3,300 cm^{-1}). Therefore, the obtained IR data indicated that all four catalysts had proper functional groups, thereby confirming that the catalysts were synthesized as expected.

2. NMR Analysis of the Solid-type Catalysts

Solid-state nuclear magnetic resonance (NMR) spectroscopy with ^{13}C with cross-polarization (CP) and magic angle spinning (MAS) (CPMAS ^{13}C NMR) was used to characterize the catalysts [39]. ^{13}C CP NMR spectra were obtained on an AVANCE III HD (Bruker, Germany) spectrometer operating at 100.66 MHz. The basic specifications and conditions were as follows: 400 MHz solid state (C) NMR (9.4 T), MAS spinning rate of 10 kHz, chemical shifts measured in reference to TMS (0 ppm), and room temperature (25 °C). Samples were packed in a zirconia rotor (OD=4 mm) and spun at 5 kHz at the magic angle. A total of 15000 transients were collected over a sweep width of 10 kHz. In some instances, it was necessary to further divide some of the chemical shift regions: O-alkyl C into methoxyl C (50-60 ppm), carbohydrate C (60-90 ppm), and di-O-alkyl C (90-110 ppm), and aromatic C into aryl C (110-142 ppm) and phenolic C (142-160 ppm) [40]. The basic peak positions of Solid NMR and Solution NMR are the same. But the degree of broadness is different. Since there is no polymer having the same structure as the synthesized solid catalyst, it was difficult to assign the peak according to some reference. A similar type of polymer can be found in the related patent [41], which can be interpreted as a solid NMR analysis suitable for the structure of the solid cata-

lyst in Fig. 4.

The solid state ^{13}C NMR NMR spectra of the catalysts are presented in Fig. 4. As can be seen, the peak for piperazinediol appeared broad between 40 and 80 ppm (Fig. 4(a)). In contrast, triol piperazine showed several peaks, with that of terminal $\underline{C}H_3$ appearing at 7.71 ppm, that of central $\underline{C}C_4$ among the three piperazines showing sharp at 45.4 ppm, and the remainder forming a broad peak between 50 and 80 ppm (Fig. 4(b)). In Fig. 4(c), the three characteristic peaks of the aromatic ring in triphenylpiperazine appeared in 117.29, 131.59, 140.4 and 159.16 ppm, while the remainder could be seen between 40 and 70 ppm. Moreover, the C=O peak of cyanupiperazine was detected at 151.4 ppm, with the other peaks appearing between 40 and 70 ppm (Fig. 4(d)). Although the peaks of the solid ^{13}C NMR spectra were broad, their positions were as expected. Therefore, these results combined with the FT-IR data verified that the solid catalysts were well-formed and contained the proper functional groups.

3. Experimental Tests of the Solid-type Catalysts

When a metal halide catalyst is used as a homogeneous catalyst, its activity depends on the Lewis acidity of the cation, nuclear affinity of the anion at low pressure, and the solubility of the catalyst. Unlike metal halide catalysts, the reaction mechanism involving homogeneous multifunctional alkanolamine catalysts could be affected by the synergy effect of hydroxyl and amine groups. Although a small amount of water can increase the yield by promoting the cycloaddition reaction of the amine catalyst, the use of alkanolamine is more effective and the selectivity is lowered by the side reaction [42]. The hydroxyl groups are suggested to strongly interact with epoxides, thus facilitating their ring opening by bringing amine-bound CO_2 into proximity with the electrophilic center. Moreover, the lone pair of electrons on the catalyst nitrogen atom is thought to interact with the electrophilic carbon of CO_2, thereby

Table 1. Cycloaddition reaction results using solid type catalysts (10 bar, 120 $^{\circ}$C, 3 h)

Catalyst	Reactant	Yield (%)	Selectivity (%)
Piperazinediol	Propylene oxide	96	>99
	Styrene oxide	91	>99
	Epichlorohydrin	89	>99
	Cyclohexene oxide	12	>99
	Allyl glycidyl ether	90	>99
Triepoxypiperazine	Propylene oxide	92	>99
	Styrene oxide	83	>99
	Epichlorohydrin	82	>99
	Cyclohexene oxide	9	>99
	Allyl glycidyl ether	80	>99
Triphenylepoxypiperazine	Propylene oxide	76	>99
	Styrene oxide	72	>99
	Epichlorohydrin	72	>99
	Cyclohexene oxide	7	>99
	Allyl glycidyl ether	71	>99
Cyanupiperzine	Propylene oxide	63	>99
	Styrene oxide	55	>99
	Epichlorohydrin	56	>99
	Cyclohexene oxide	5	>99
	Allyl glycidyl ether	54	>99

[a]PO=5 g, amount of catalyst=1.0 g

Table 2. Cycloaddition reaction results using piperazinediol under various reaction conditions

	[a]Reaction conditions	Amount of catalyst (g)	Yield (%)	Selectivity (%)
Piperazinediol	120 $^{\circ}$C, 3 h	0.5	76	>99
	100 $^{\circ}$C, 3 h	3.0	93	>99
	70 $^{\circ}$C, 24 h	3.0	71	>99
	60 $^{\circ}$C, 24 h	3.0	52	>99

[a]PO=5 g, CO_2=10 bar

Table 3. Cycloaddition reaction results using solid type catalysts

	[a]Reaction condition	Yield (%)	Selectivity (%)
1st Reaction test	60 $^{\circ}$C, 24 h, 3.0 g	52	>99
2nd Regeneration		52	>99
3rd Regeneration		51	>99
4th Regeneration		51	>99
5th Regeneration		50	>99

[a]PO=5 g, CO_2=10 bar

promoting the nucleophilic attack of the CO_2 oxygen atom on the alkyl oxide and allowing its ring opening [21]. The four solid-type catalysts were subsequently used in the cycloaddition reaction between CO_2 and oxyranes (propylene oxide, styrene oxide, epichlorohydrin, cyclohexene oxide and allyl glycidyl ether (Table 1)) under the following conditions. Reaction time: 3 h, CO_2 pressure: 10 bar, PO amount: 5 g, and reaction temperature: 120 $^{\circ}$C.

Catalyst 1 was the most excellent among the four solid-type catalysts, because it was the continuous form of the piperazinediol, which was the most excellent in the previous paper [21]. Catalyst 1 was synthesized using piperazine in the form of a primary amine at both ends instead of methyl piperazine used in synthesizing the piperazinediol in order to make a continuous form of the piperazinediol. In the tested catalysts, piperazinediol and triepoxypiperazine gave better results, which could be explained with the aforementioned homogeneous alkanolamine catalyst mechanism involving the synergistic effects of the amine and hydroxyl groups [21]. Since triphenylepoxypiperazine and cyanupiperazine have rigid structures such as piperazine and benzene, it would be difficult for two functional groups to be brought together. In contrast, piperazinediol and triepoxypiperazine are flexible at high temperatures, so synergistic effects between the amine and hydroxyl groups can be expected.

As shown in Table 2, the piperazinediol catalyst, which gave the best yield, was applied at low reaction temperatures of 100, 70, and 60 $^{\circ}$C. GC analysis showed that 93% product yield was obtained after 3 h at 100 $^{\circ}$C, and 71% and 60% yields were achieved after 24 h

at 70 and 60 $^{\circ}$C, respectively. These reactions also exhibited high selectivity, which was determined from the fact that no by-products were detected. When the reaction was at 100 $^{\circ}$C, the catalyst amount was increased to 3 g to counteract the low-temperature reaction. At mild temperatures (60 and 70 $^{\circ}$C) the reaction time was prolonged to 24 h.

Next, the catalyst regeneration ability of piperazinediol (3 g) was tested under the following conditions (Table 3). CO_2 pressure: 10 bar, reaction temperature: 60 $^{\circ}$C, and reaction time: 24 h. Notably, the catalyst was easily separated from the mixture of the product and unreacted materials, as it was solid. Moreover, since the yield was maintained at 52-50 $^{\circ}$C when the reaction was repeated five times, we concluded that the catalyst could be regenerated. Despite the long reaction times and large catalyst amount, having a moderate yield at mild temperatures (60 $^{\circ}$C) is significant.

CONCLUSION

Efforts to employ metal- and halogen-free catalysts in CO_2 cycloaddition reactions, combined with the use of heterogeneous catalysts, is environmentally and commercially important. We prepared four metal- and halogen-free solid organic catalysts and analyzed their structures via ^{13}C solid-state NMR and FT-IR. In addition, we evaluated their performance in a CO_2 cycloaddition reaction and obtained 98% product yield after 3 h at 120 $^{\circ}$C. At a mild reaction temperature (60 $^{\circ}$C), 50% yield was obtained and the catalyst was successfully regenerated. Moreover, at this temperature, the obtained polymer-type catalyst could be re-used up to five times without any significant performance loss. As a result, a multifunctional solid catalyst that does not contain any metal or halogen atoms, which could be recycled at low temperatures, was prepared in this study. In our future work, we are planning to investigate different applications of these catalysts for commercial use.

ACKNOWLEDGEMENTS

SUPPORTING INFORMATION

Additional information as noted in the text. This information is available via the Internet at http://www.springer.com/chemistry/journal/11814.

REFERENCES

1. T. R. Anderson, E. Hawkins and P. D. Jones, *Endeavour*, **40**, 178 (2016).
2. E. Alper and O. Y. Orhan, *Petroleum*, **3**, 109 (2017).
3. M. North, R. Pasquale and C. Young, *Green Chem.*, **12**, 1514 (2010).
4. M. Cokoja, C. Bruckmeier, B. Rieger, W. A. Herrmann and F. E. Kühn, *Angew. Chem., Int. Ed.*, **50**, 8510 (2011).
5. M. North and R. Pasquale, *Angew. Chem., Int. Ed.*, **48**, 2946 (2009).
6. W. L. Dai, S. L. Luo, S. F. Yin and C. T. Au, *Appl. Catal., A.*, **366**, 2 (2009).
7. M. Cokoja, M. E. Wilhelm, M. H. Anthofer, W. A. Herrmann and F. E. Kühn, *ChemSusChem*, **8**, 2436 (2015).
8. C. Martín, G. Fiorani and A. W. Kleij, *ACS Catal.*, **5**, 1353 (2015).
9. A. A. G. Shaikh and S. Sivaram, *Chem. Rev.*, **96**, 951 (1996).
10. T. Sakakura and K. Kohno, *Chem. Commun.*, 1312 (2009).
11. S. Y. Huang, S. G. Liu, J. P. Li, N. Zhao, W. Wei and Y. H. Sun, *Fuel Chem. Technol.*, **35**, 701 (2007).
12. B. M. Bhanage, S.-i. Fujita, Y. Ikushima and M. Arai, *Appl. Catal. A*, **219**, 259 (2001).
13. D. Bai, S. Duan, L. Hai and H. Jing, *ChemCatChem*, **4**, 1752 (2012).
14. J. Zhang, X. Cheng, B. Zhang, J. Shi, L. Zheng, J. Zhang, D. Shao, X. Tan, B. Han and G. Yang, *ChemCatChem*, **10**, 1 (2018).
15. J. Song, Z. Zhang, B. Han, S. Hu, W. Li and Y. Xie, *Green Chem.*, **10**, 1337 (2008).
16. L. N. He, H. Yasuda and T. Sakakura, *Green Chem.*, **5**, 92 (2003).
17. A. Decortes, A. M. Castilla and A. W. Kleij, *Angew. Chem., Int. Ed.*, **49**, 9822 (2010).
18. Y. Zhang and J. Y. G. Chan, *Energy Environ. Sci.*, **3**, 408 (2010).
19. M. O. Vieira, W. F. Monteiro, B. S. Neto, R. Ligabue, V. V. Chaban and S. Einloft, *Catal. Lett.*, **148**, 108 (2018).
20. P. Wasserscheid and T. Welton, *Ionic Liquids in Synthesis*, 2nd Ed., Wiley-VCH (2008).
21. H.-G. Kim, C. S. Lim, D. W. Kim, D.-H. Cho, D. K. Lee and J. S. Chung, *Mol. Catal.*, **438**, 121 (2017).
22. J. Chen, M. Zhong, L. Tao, L. Liu, S. Jayakumar, C. Li, H. Li and Q. Yang, *Green Chem.*, **20**, 903 (2018).
23. S. Wu, C. Teng, S. Cai, B. Jiang, Y. Wang, H. Meng and H. Tao, *Nanoscale Res. Lett.*, **12**, 1 (2017).
24. L. X. Wu, H. P. Yang, Y. B. Guan, M.-P. Yang, H. Wang and J. X. Lu, *Int. J. Electrochem. Sci.*, **12**, 8963 (2017).
25. D.-H. Lan, Y.-X. Gong, N.-Y. Tan, S.-S. Wu, J. Shen, K.-C. Yao, B. Yi, C.-T. Au and S.-F. Yin, *Carbon*, **127**, 245 (2018).
26. D.-H. Lan, H.-T. Wang, L. Chen, C.-T. Au and S.-F. Yin, *Carbon*, **100**, 81 (2016).
27. D.-H. Lan, L. Chen, C.-T. Au and S.-F. Yin, *Carbon*, **93**, 22 (2015).
28. D.-H. Lan, F.-M. Yang, S.-L. Luo, C.-T. Au and S.-F. Yin, *Carbon*, **73**, 351 (2014).
29. Z. Z. Yang, Y. N. Zhao and L. N. He, *RSC Adv.*, **1**, 545 (2011).
30. J. Sun, W. Cheng, W. Fan, Y. Wang, Z. Meng and S. Zhang, *Catal. Today*, **148**, 361 (2009).
31. A. H. Jadhav, G. M. Thorat, K. Lee, A. C. Lim, H. Kang and J. G. Seo, *Catal. Today*, **265**, 56 (2016).
32. R. F. Sammelson and M. J. Kurth, *Chem. Rev.*, **101**, 137 (2001).
33. A. Chen, Y. Zhang, J. Chen, L. Chen and Y. Yu, *J. Mater. Chem. A*, **3**, 9807 (2015).
34. X.-L. Meng, Y. Nie, J. Sun, W.-G. Cheng, J.-Q. Wang, H.-Y. He and S.-J. Zhang, *Green Chem.*, **16**, 2771 (2014).
35. S. N. Talapaneni, O. Buyukcakir, S. H. Je, S. Srinivasan, Y. Seo, K. Polychronopoulou and A. Coskun, *Chem. Mater.*, **27**, 6818 (2015).
36. J. Roeser, K. Kailasam and A. Thomas, *ChemSusChem*, **5**, 1793 (2012).
37. R. Skelton, F. Dubois and R. Zenobi, *Anal. Chem.*, **72**, 1707 (2000).
38. N. A. Rangel-Vazquez, C. Sánchez-López and F. R. Felix, *Polímeros*, **24**, 453 (2014).
39. N. J. Mathers and Zhihong Xu, *Geoderma*, **114**, 19 (2003).
40. B. Ochiai and T. Endo, *Prog. Polym. Sci.*, **30**, 183 (2005).
41. D. A. Tomalia, D. R. Swanson, B. Huang, S. Svenson, L. A. Reyna, Michael A, C. R. DeMattei and J. R. Heinzelmann, US Patent, 0298006A1 (2007).
42. K. R. Roshan, B. M. Kim, A. C. Kathalikkattil, J. Tharun, Y. S. Won and D. W. Park, *Chem. Commun.*, **50**, 13664 (2014).

Supporting Information

Metal- and halide-free solid-type multifunctional alkanolamines as catalysts for cycloaddition of CO$_2$

Hyeon-Gook Kim[†], Hye Jeong Son, and Choong-Sun Lim

Advanced Industrial Chemistry Research Center, Advanced Convergent Chemistry Division,
Korea Research Institute of Chemical Technology, 45 Jongga-ro, Jung-gu, Ulsan 44412, Korea

EXPERIMENTAL

1. MAILDI-TOF Analysis of Solid Catalysts
  <Characterization method of MAILDI-TOF>
1-1. MS Conditions
  Operating Mode: MS Reflector mode (Positive)
  Mass Range (m/z): 1,000-3,000 Da

1-2. MALDI Marix
  2,5-Dihydroxybenzoic acid (DHB): 10 mg/mL (water)
  2,5-Dihydroxybenzoic acid (DHB): 10 mg/mL (THF)
  Dithranol: 10 mg/mL (THF/0.1% TFA)
1-3. MS Calibration Mixture
  Arg1-Bradykinin (904.468)
  Angiotensin I (1296.685)

Fig. S1. (a) MALDI-TOF of piperazinediol catalyst. (b) MALDI-TOF of piperazinediol catalyst.
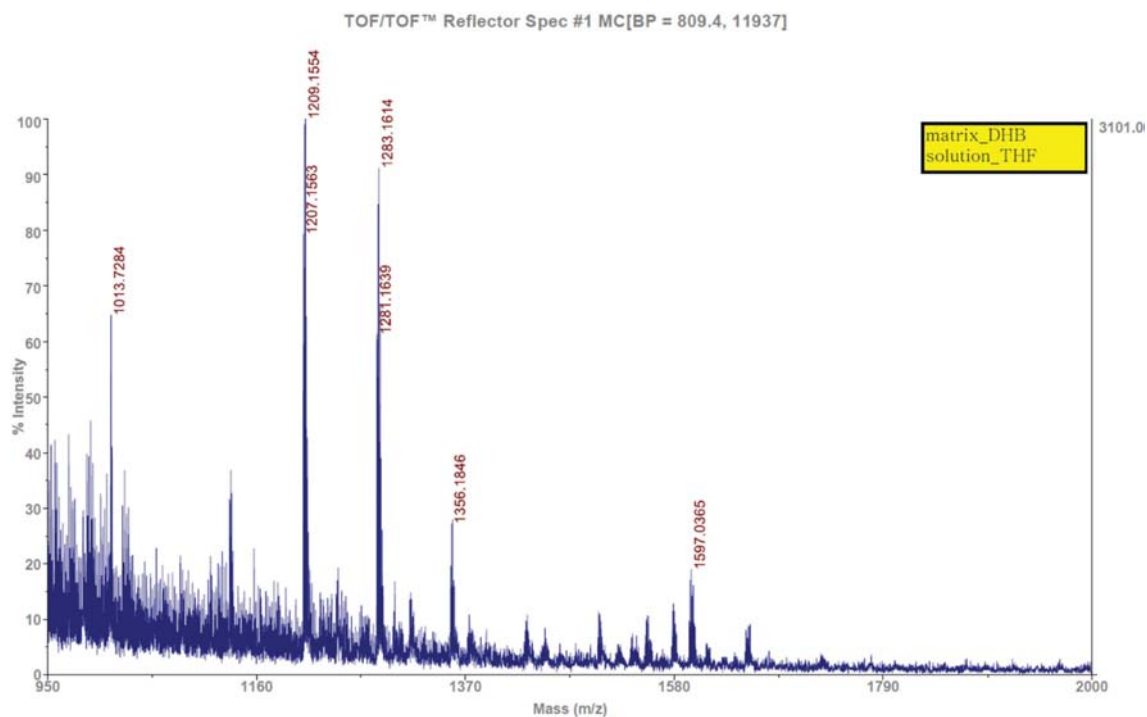
Fig. S2. MALDI-TOF of triolpiperazine catalyst.

Glu1-Fibrinopeptide B (1570.677)
ACTH (1-17) (2093.087)
ACTH (18-39) (2465.199)
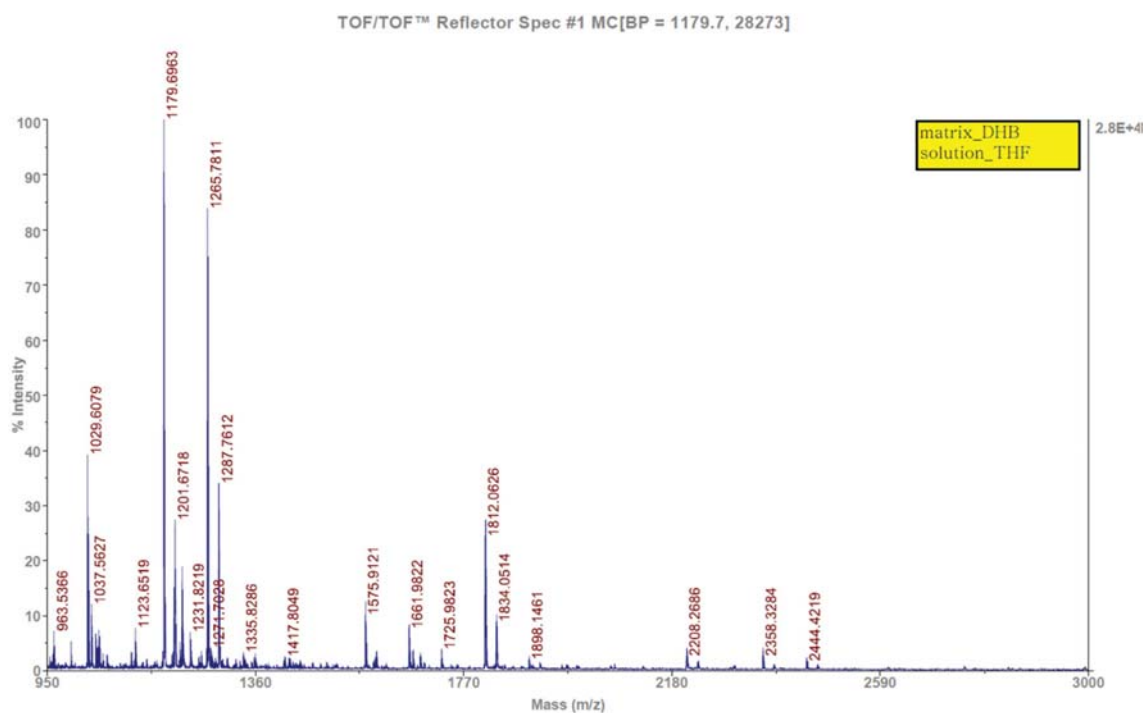ACTH (7-38) (3657.9294)
MS calibration: 50 ppm
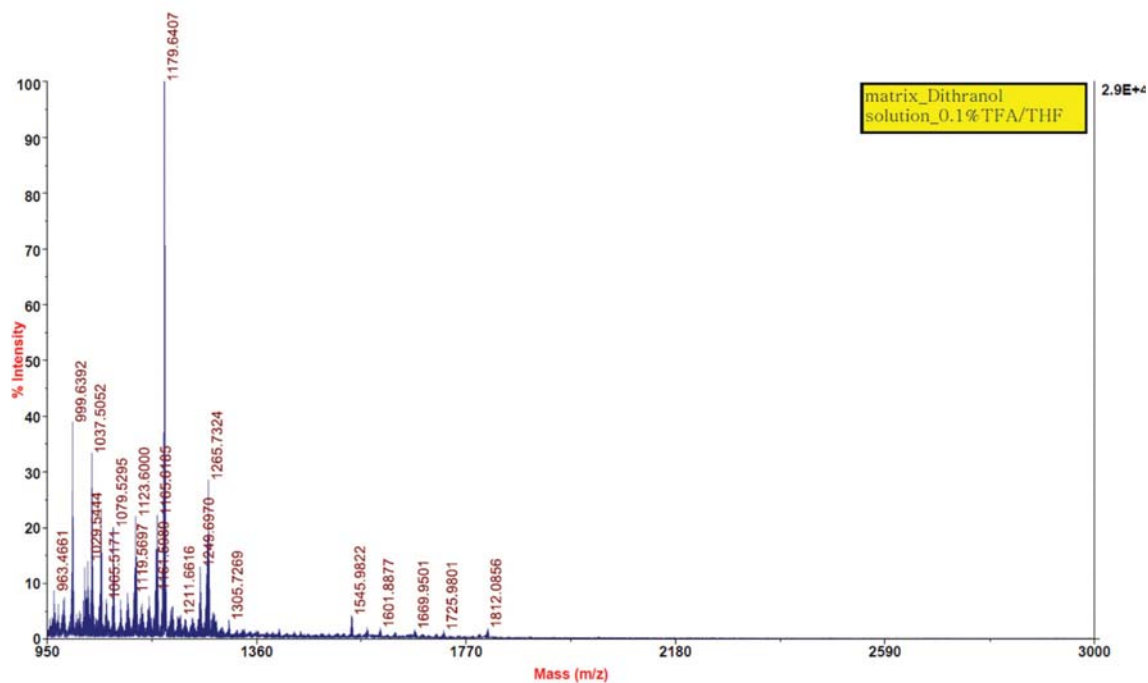1-4. Data Processing
   - Baseline correction

- Noise filter/smooth (Gaussian smooth 5 points)
1-5. Sample Preparations
   1) preparation matrix
   2) make sample: matrix=1 : 1 (w/w) add in matrix solution.
   3) sonication for 1 h
   4) do spin-down and plate loading upper layer

(a)

(b)

Fig. S3. (a) MALDI-TOF of triphenylpiperazine catalyst. (b) MALDI-TOF of triphenylpiperazine catalyst.
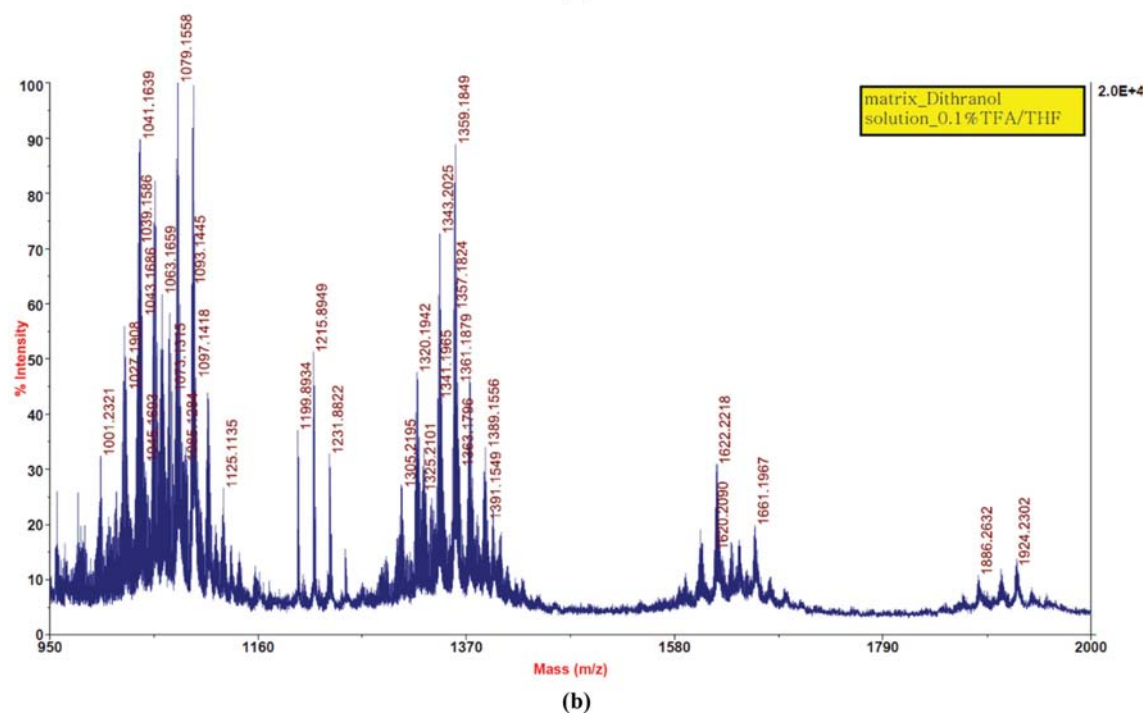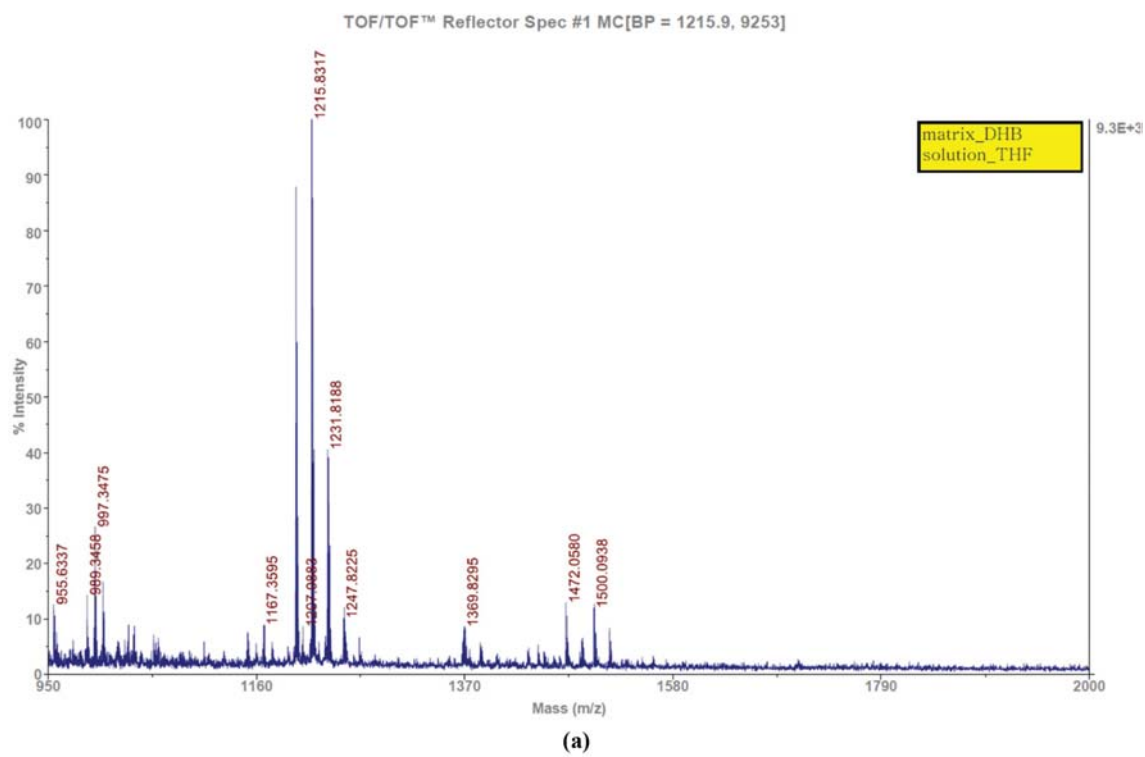
Fig. S4. (a) MALDI-TOF of cyanupiperazine catalyst. (b) MALDI-TOF of cyanupiperazine catalyst.